Conversion of Polystyrene to Terephthalic Acid via Sequential Acetylation and Mn/Br-Catalyzed Autoxidation

Doohyun Baek,[a,b] Dylan J. Walsh,[a,b] James B. Gerken,[a] Madelyn G. Frank,[a] Ive Hermans,[a,b,c] Shannon S. Stahl[a,b]*

[a]Department of Chemistry, University of Wisconsin−Madison, Madison, Wisconsin 53706, United States

[b]The Wisconsin Energy Institute, University of Wisconsin−Madison, Madison, Wisconsin 53726, United States

[c]Department of Chemical and Biological Engineering, University of Wisconsin−Madison, Madison, Wisconsin 53706, United States

KEYWORDS: polymer, recycling, upcycling, aerobic, Mid-Century Process

ABSTRACT: Most methods for oxidative deconstruction of polystyrene produce benzoic acid, which has a low market size relative to the production of waste polystyrene. The present study demonstrates a method for conversion of polystyrene into terephthalic acid, a high-volume chemical, by introducing a carbon-containing fragment into the *para* position of the phenyl groups in polystyrene, followed by Mn/Br-catalyzed autoxidation. Acetylated polystyrene is shown to be the most effective substrate for oxidation, affording an 81% yield of terephthalic acid. Mechanistic studies highlight the effectiveness of bromide as a cocatalyst and offer insight into the underlying reasons the acetyl group undergoes efficient oxidation.

INTRODUCTION

Polystyrene (PS) is among the top five highest volume polymers produced globally, but it is rarely recycled after use, with the majority going to landfills.[1] Aerobic oxidation methods offer a potential strategy for chemical recycling of PS,[2,3] as they are thermodynamically favorable, have potential to tolerate impurities or additives, and can generate value-added products that can re-enter the chemical value chain. Most existing methods for oxidation of PS generate benzoic acid (**Figure 1a**);[4–7] however, the comparatively small market demand of benzoic acid motivates efforts to access alternative products, such as phenol,[8] or to develop integrated processes that convert benzoic acid into other products via bioconversion.[5,9] Terephthalic acid (TA), a high-volume monomer used to make poly(ethylene terephthalate) (PET), represents an appealing target for waste PS valorization. It is produced industrially by liquid-phase oxidation of *p*-xylene using a multicomponent Co/Mn/Br catalyst system, commonly known as the Mid-Century (MC) process (**Figure 1b**).[10,11] We postulated that selective introduction of a methyl group or another carbon-containing substituent onto the aromatic rings of PS could enable selective oxidative conversion of the modified PS into TA (**Figure 1c**). This strategy would resemble the industrial process for conversion of toluene into terephthalic acid via selective methylation of toluene to access *p*-xylene,[12] prior to oxidation in the MC process. During our exploration of this strategy, De Vos and co-workers reported a successful implementation of this concept.[13] They introduced acetyl or isopropyl groups onto the phenyl rings of PS and subsequently oxidized the modified polymers using a Mn/N-hydroxyphthalimide (NHPI) catalyst system (4/60 wt%, respectively). Their best results were obtained with acetylated

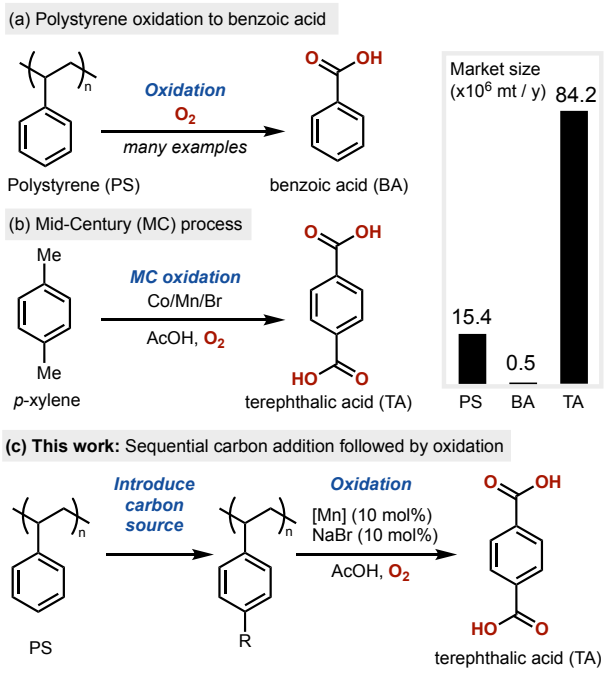

Figure 1. (a) Oxidative degradation of polystyrene (PS) typically yields benzoic acid. (b) Mid-Century process for industrial production of terephthalic acid from *p*-xylene using Co/Mn/Br catalysis. (c) The proposed strategy involves functionalizing PS with a carbon-containing group, enabling its subsequent oxidative transformation into terephthalic acid.

PS, which afforded terephthalic acid (TA) in yields up to 55%, along with phthalic acid derived from NHPI hydrolysis. In our parallel studies, we find that bromide offers significant advantages over NHPI as a cocatalyst. We also systematically evaluate a range of carbon-containing substituents and identify the acetyl group as particularly effective when paired with a Mn/Br-based oxidation catalyst. In line with the findings of De Vos and co-workers, we observe that acetylated PS is a highly efficient substrate, achieving an 81% yield of TA under our optimized conditions. Mechanistic studies further elucidate the key features that contribute to the high efficiency of the Mn/Br catalytic system.

RESULTS AND DISCUSSION

The present study was initiated in parallel with our recent investigation of NHPI-mediated autoxidation of PS to generate phenol.[8] NHPI is well-established as a hydrogen-atom-transfer mediator in hydrocarbon autoxidation,[14–16] including reactions with PS.[5,8,9,13,17,18] NHPI can be used as a substitute for bromide in MC oxidations, avoiding the need for specialized corrosion-resistant reactors;[19] however, the oxidized state of NHPI, phthalimide *N*-oxyl (PINO), has poor stability and undergoes ring-opening decomposition at elevated temperatures.[15,16,20–22] These considerations prompted us to compare Mid-Century (MC)-type oxidation conditions using either NHPI or bromide as a cocatalyst. Specifically, two experiments were conducted with cumene as a model compound for PS at 140 °C with 100 psi O_2 in AcOH, employing either a Co/Mn/NHPI or Co/Mn/Br catalyst system (**Figure 2**; see Section 1c of the Supporting Information for safety considerations because the conditions fall within the flammability region of acetic acid and O_2[23,24]). Reactions were monitored by gas chromatography–mass spectrometry with flame ionization detection (GC-MS/FID). In both cases, cumene was rapidly converted, and acetophenone (ACP) was observed as an intermediate *en route* to benzoic acid. In the NHPI-catalyzed reaction, NHPI was consumed within 10 minutes, and ACP did not fully convert to benzoic acid, resulting in a stalled yield of 77% (**Figure 2**, left). In contrast, when NaBr was used as a cocatalyst, cumene underwent more rapid and nearly quantitative conversion to benzoic acid. These results are consistent with the known thermal instability of NHPI and suggest that, under these conditions, NHPI acts more as a 'radical initiator' than as a true 'mediator' or 'cocatalyst'.

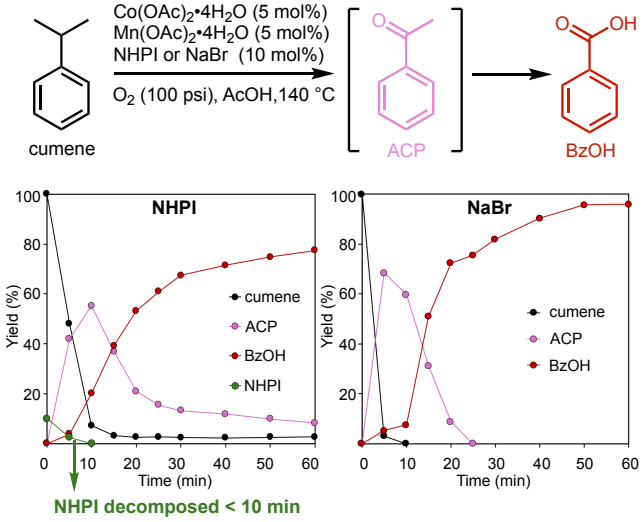

Figure 2. Comparison between NHPI (left) and NaBr (right) as cocatalysts in Co/Mn-catalyzed oxidation of cumene.

The superior performance observed with bromide led us to adopt bromide-based systems in subsequent studies. We then sought to identify the carbon-based fragments that could be introduced into PS for conversion to TA under MC oxidation conditions. These efforts were initiated with cumene-derived model compounds, with *para* substituents including methyl (**1**), bromomethyl (**2**), chloromethyl (**3**), formyl (**4**), and acetyl (**5**) groups (**Figure 3a**). Methods to introduce each of these substituents are known in the literature.[12,25–32] MC oxidation conditions with reduced catalyst loading (2/2/4 mol% Co/Mn/Br) were adopted to accentuate the differences between

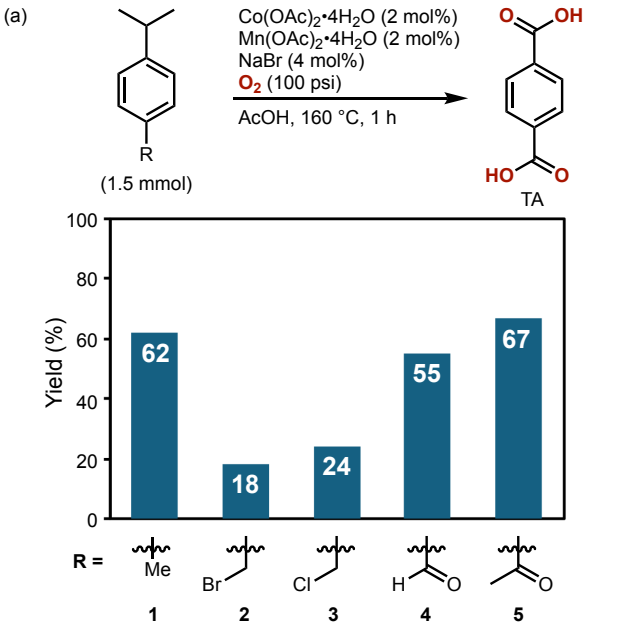

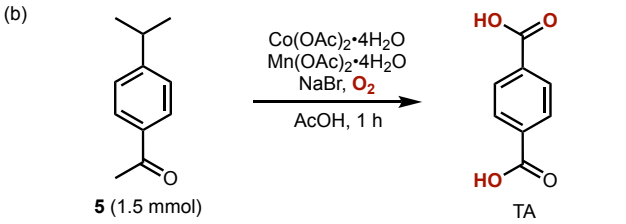

Entry	Catalysts [mol%]	Conc. [M]	O_2 condition	Temp. [°C]	Yield[a] [%]
1	Co/Mn/Br = 5/5/10	0.1	100 psi	160	71
2	Mn/Br = 10/10	0.1	100 psi	160	76
3	Mn/Br = 10/10	0.3	100 psi	160	79
4	Mn/Br = 10/10	0.3	100 psi	180	81
5[b]	Mn/Br = 10/10	0.3	200 psi	180	82

Figure 3. (a) Evaluation of carbon-containing substituents for MC oxidation to produce terephthalic acid. (b) Optimization of autoxidation conditions using compound 5 as a model substrate. [a]Isolated yield. [b]The reaction was carried out on a 30 mmol scale of 5 using titanium Parr reactor. Reaction conditions: 1.5 mmol or 30 mmol of 5, 5 mol% of $Co(OAc)_2•4H_2O$, 5 or 10 mol% of $Mn(OAc)_2•4H_2O$, 10 mol% of NaBr, O_2 (100 or 200 psi) in AcOH at 140 °C or 180 °C.

the different substrates. As expected, the methyl derivative **1** underwent efficient oxidation, affording TA in 62% yield, while lower yields were observed with the halomethyl derivatives **2** and **3**. The formyl and acetyl derivatives **4** and **5** showed good reactivity, with the highest yield observed with acetyl (67%). We therefore focused on optimization of MC conditions for oxidation of **5** (**Figure 3b**). Each of the catalyst components was evaluated, in addition to consideration of reaction concentrations, temperatures, and O_2 pressures (see section 3b of Supporting Information for full reaction screening data). The most notable outcome of these studies was the observation that cobalt had little impact on the reaction outcome.[33] Optimal results could be accessed with a Mn/Br-based catalyst system, affording 82% yield of TA with 0.3 M substrate concentration at 180 °C and 200 psi O_2 (entry 5, **Figure 3b**).

These optimized conditions were then applied to the oxidation of acetylated polystyrene (AcPS). Conditions reported previously in the literature were used for PS acetylation, using aluminum chloride ($AlCl_3$) and acetyl chloride (AcCl) in CS_2 as a solvent.[30–32] These conditions led to acetylation of 95% of the phenyl groups in PS (**Figure 4a**), as determined by ^{1}H NMR analysis of the resulting polymer (**Figure 4b**; see section 4a in the Supporting Information for further discussion). IR spectra of the AcPS showed a strong C=O stretch peak at 1680 cm^{-1} and a C-(C=O)-C bend peak at 1269 cm^{-1} (**Figure 4c**). These peaks are similar to the IR spectra of acetophenone (ACP), consistent with incorporation of acetyl group on the phenyl groups of PS. GPC analysis revealed that there is no significant change in the molecular weight between PS and AcPS, indicating that acetylation does not induce chain-scission or cross-linking (**Figure 4d**). Literature precedents raised the possibility of catalytic Friedel-Crafts acylation,[34–37] but attempted reactions with PS were unsuccessful (see Table S2 for details). Acetylation of polystyrene with ethenone (i.e., ketene) has been demonstrated with substoichiometric (33 mol%) $AlCl_3$[30] and could be considered for large scale applications.

The AcPS was then subjected to the optimized MC oxidation conditions. The highest yield of TA (81% with respect to acetylated phenyl rings) was observed after 4 h (**Figure 4e**). This outcome represents an improvement over the 55% yield of TA obtained with a Mn/NHPI catalyst system,[13] aligning with the improved performance of bromide relative to NHPI in the reaction of cumene in **Figure 2**.

These observations, together with the previous observations of De Vos and coworkers,[13] prompted us to consider the origin of the favorable reactivity of an acetyl group in this process. To probe this issue, we compared the reactivity of substrates **1** and **5**, which feature a *para*-methyl or -acetyl group in cumene, under the optimized Mn/Br oxidation conditions (**Figure 5**).[38] Time-course data with both substrates were obtained from GC-MS/FID analysis and revealed that both reactions undergo initial oxidative conversion of the isopropyl group into an acetyl group, forming 1,4-diacetylbenzene **5a** (**Figure 5a** and Figure S5a) or *p*-methylacetophenone **1a** (**Figure 5b** and Figure S5b). The acetyl group is then converted to a carboxylic acid, affording *p*-acetylbenzoic acid **5c** and *p*-toluic acid **1b**, respectively. TA is not soluble under the reaction conditions, and it was quantified following filtration after stopping the reaction (71% yield of TA from **5** and 53% yield from **1**, after 60 min). In addition to these major pathways, minor pathways

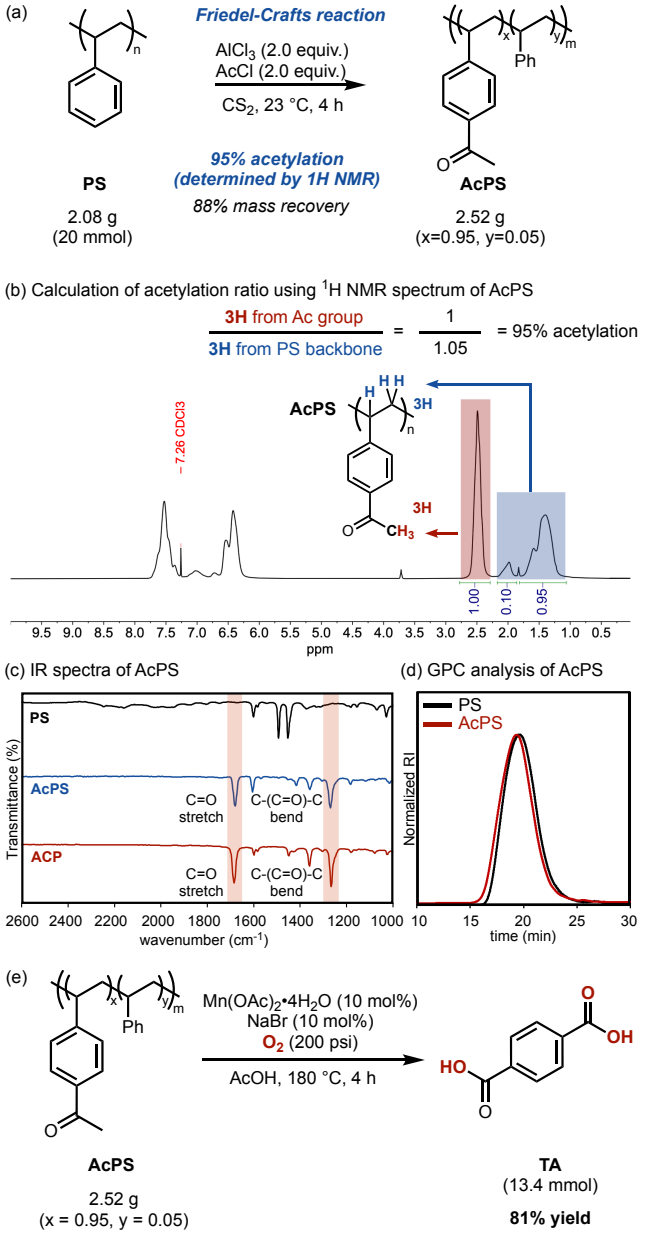

Figure 4. Sequential acylation/oxidation of polystyrene to produce terephthalic acid. (a) Synthesis of acetylated polystyrene (AcPS). Reaction conditions: 2.08 g of PS, 40 mmol of $AlCl_3$, 40 mmol of AcCl in CS_2 at 23 °C for 4 h. (b) Calculation of acetylation ratio based on ^{1}H NMR spectra of AcPS. (c) IR spectra of AcPS. (d) GPC analysis of starting PS and AcPS. (e) Application of Mn/Br oxidation conditions to AcPS. Catalyst mol% loading is defined with respect to the total aromatic subunits in AcPS.

are also evident in the reactions, leading to the formation of *p*-isopropylbenzoic acid **5b** via oxidation of the acetyl group in **5** or the methyl group in **1**.

Collectively, these data reveal significantly less build-up of reaction intermediates in the reaction of **5** relative to the reaction of **1**. In the former case, only the diacetyl derivative **5a** accumulates to a significant extent. The negligible formation of **5b** shows that oxidation of the isopropyl group in **5** is more facile than oxidation of the acetyl group (**Figure 5a**); however, the minor accumulation of **5c** shows that the acetyl group is also

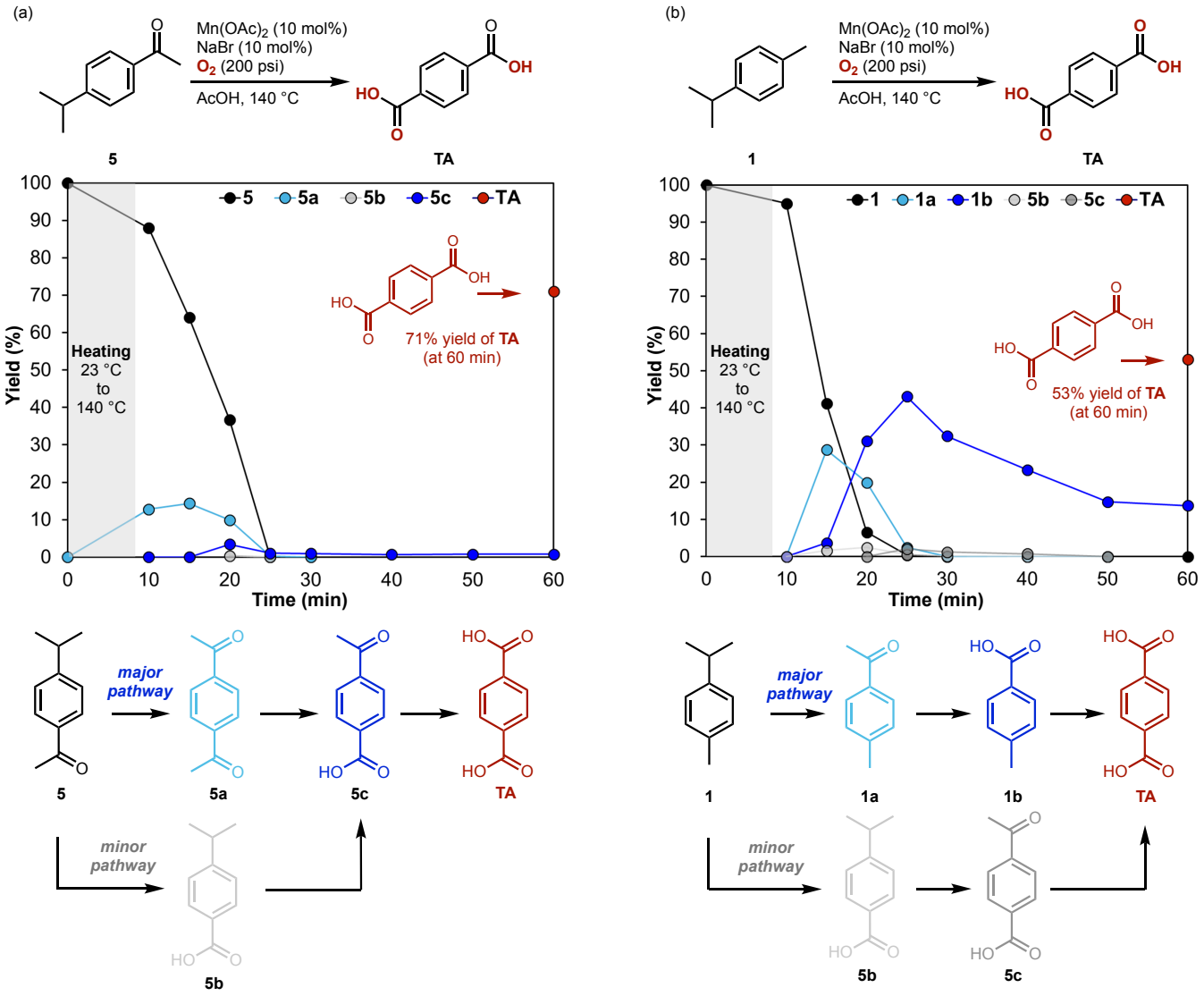

Figure 5. Time-course reaction profile of the oxidation reaction of **5** (a) and **1** (b). The heating zone represents the period required for the titanium reactor to reach 140 °C. Reaction conditions: 10 mmol of **1** or **5**, 10 mol% of $Mn(OAc)_2•4H_2O$, 10 mol% of NaBr, O_2 (200 psi) in 100 mL of AcOH at 140 °C using a titanium Parr reactor.

readily oxidized. In contrast, the reaction of **1** shows significant build-up of intermediates **1a** and **1b**. Preferential oxidation of the isopropyl group over the methyl group in **1** aligns with the relative bond dissociation energies of 3° and 1° C–H bonds.[39] The least reactive intermediate in the conversion of **1** to TA is *p*-toluic acid **1b**, which does not undergo complete conversion after 1 h (**Figure 5b**). *p*-Toluic acid has also been identified as a problematic intermediate in the industrial MC oxidation of *p*-xylene to TA.[10] These results with substrates **5** and **1** suggest that the favorable reactivity of AcPS occurs by the good oxidative reactivity of the acetyl group under the Mn/Br conditions and avoidance of problematic intermediates analogous to **1b**.

CONCLUSION

The results presented here establish improved conditions for conversion of polystyrene (PS) into terephthalic acid (TA), a high-volume commodity chemical produced at a scale suitable for waste PS recycling. We demonstrate that bromide is a more effective cocatalyst rather than NHPI, significantly enhancing the yield of TA that can be accessed from AcPS and avoiding byproducts associated with NHPI degradation during the reaction. Time-course analysis highlights the facile oxidative conversion of the acetyl group into a carboxylic acid. These observations, together with the observation that cobalt is not needed to promote efficient reactivity, are the focus of an ongoing mechanistic study.

AUTHOR INFORMATION

Corresponding Author

Shannon S. Stahl – Department of Chemistry, University of Wisconsin-Madison, Madison, Wisconsin 53706, United States; The Wisconsin Energy Institute, University of Wisconsin-Madison, Madison, Wisconsin 53726, United States; orcid.org/0000-0002-9000-7665; Email: stahl@chem.wisc.edu

Present Addresses

Doohyun Baek – Department of Chemistry, University of Wisconsin-Madison, Madison, Wisconsin 53706, United States; The Wisconsin Energy Institute, University of Wisconsin-Madison, Madison, Wisconsin 53726, United States; orcid.org/ 0000-0003-4059-2832
Dylan J. Walsh− Department of Chemistry, University of Wisconsin-Madison, Madison, Wisconsin 53706, United States; The Wisconsin Energy Institute, University of Wisconsin-Madison, Madison, Wisconsin 53726, United States; orcid.org/0000-0001-7981-2770
James B. Gerken – Department of Chemistry, University of Wisconsin–Madison, Madison, Wisconsin 53706, United States; orcid.org/0009-0000-9294-6300
Madelyn G. Frank – Department of Chemistry, University of Wisconsin–Madison, Madison, Wisconsin 53706, United States;
Ive Hermans – Department of Chemistry, University of Wisconsin-Madison, Madison, Wisconsin 53706, United States; The Wisconsin Energy Institute, University of Wisconsin-Madison, Madison, Wisconsin 53726, United States; Department of Chemical and Biological Engineering, University of Wisconsin−Madison, Madison, Wisconsin 53706, United States; orcid.org/0000-0001-6228-9928

Notes

The authors declare no competing financial interests.

ASSOCIATED CONTENT

Supporting Information

The Supporting Information is available free of charge at XYZ.

Experimental details with supplemental notes, characterization data and NMR spectra (PDF)

ACKNOWLEDGMENT

We thank Dr. Dillon Hofsommer (UW-Madison) for helpful discussions. This work was supported by the DOE Office of Science (Office of Basic Energy Sciences) grant DE-SC0023281. NMR spectrometers were supported by the NSF grant CHE-1048642 and by the Great Lakes Bioenergy Research Center (GLBRC) grant DE-SC0018409.

REFERENCES

(1) *Advancing Sustainable Materials Management: 2018 Tables and Figures*; Environmental Protection Agency, 2020.
(2) Oh, S.; Stache, E. E. Recent Advances in Oxidative Degradation of Plastics. *Chem. Soc. Rev.* **2024**, *53*, 7309–7327. https://doi.org/10.1039/D4CS00407H.
(3) Lim, J. Y. C. Low-Temperature Catalytic Approaches for Upcycling Plastics into Oxygenated Aromatic Compounds. *ChemCatChem* **2025**, *17*, e202401626. https://doi.org/10.1002/cctc.202401626.
(4) Partenheimer, W. Valuable Oxygenates by Aerobic Oxidation of Polymers Using Metal/Bromide Homogeneous Catalysts. *Catal. Today* **2003**, *81*, 117–135. https://doi.org/10.1016/S0920-5861(03)00124-X.
(5) Sullivan, K. P.; Werner, A. Z.; Ramirez, K. J.; Ellis, L. D.; Bussard, J. R.; Black, B. A.; Brandner, D. G.; Bratti, F.; Buss, B. L.; Dong, X.; Haugen, S. J.; Ingraham, M. A.; Konev, M. O.; Michener, W. E.; Miscall, J.; Pardo, I.; Woodworth, S. P.; Guss, A. M.; Román-Leshkov, Y.; Stahl, S. S.; Beckham, G. T. Mixed Plastics Waste Valorization through Tandem Chemical Oxidation and Biological Funneling. *Science* **2022**, *378*, 207–211. https://doi.org/10.1126/science.abo4626.
(6) Luo, X.; Zhan, J.; Mei, Q.; Zhang, S. Selective Oxidative Upgrade of Waste Polystyrene Plastics by Nitric Acid to Produce Benzoic Acid. *Green Chem.* **2023**, *25*, 6717–6727. https://doi.org/10.1039/D3GC00865G.
(7) Parkatzidis, K.; Wang, H. S.; Anastasaki, A. Photocatalytic Upcycling and Depolymerization of Vinyl Polymers. *Angew. Chem. Int. Ed.* **2024**, *63*, e202402436. https://doi.org/10.1002/anie.202402436.
(8) Baek, D.; Al Abdulghani, A. J.; Walsh, D. J.; Hofsommer, D. T.; Gerken, J. B.; Shi, C.; Chen, E. Y.-X.; Hermans, I.; Stahl, S. S. Can the Hock Process Be Used to Produce Phenol from Polystyrene? *J. Am. Chem. Soc.* **2025**, *147*, 8687–8694. https://doi.org/10.1021/jacs.4c18143.
(9) Rabot, C.; Chen, Y.; Lin, S.-Y.; Miller, B.; Chiang, Y.-M.; Oakley, C. E.; Oakley, B. R.; Wang, C. C. C.; Williams, T. J. Polystyrene Upcycling into Fungal Natural Products and a Biocontrol Agent. *J. Am. Chem. Soc.* **2023**, *145*, 5222–5230. https://doi.org/10.1021/jacs.2c12285.
(10) Tomás, R. A. F.; Bordado, J. C. M.; Gomes, J. F. P. *p*-Xylene Oxidation to Terephthalic Acid: A Literature Review Oriented toward Process Optimization and Development. *Chem. Rev.* **2013**, *113*, 7421–7469. https://doi.org/10.1021/cr300298j.
(11) Adamian, V. A.; Gong, W. H. Chemistry and Mechanism of Oxidation of *para*-Xylene to Terephthalic Acid Using Co–Mn–Br Catalyst. In *Liquid Phase Aerobic Oxidation Catalysis: Industrial Applications and Academic Perspectives*; John Wiley & Sons, Ltd, 2016; pp 41–66. https://doi.org/10.1002/9783527690121.ch4.
(12) Ashraf, M. T.; Chebbi, R.; Darwish, N. A. Process of *p*-Xylene Production by Highly Selective Methylation of Toluene. *Ind. Eng. Chem. Res.* **2013**, *52*, 13730–13737. https://doi.org/10.1021/ie401156x.
(13) Giakoumakis, N. S.; Marquez, C.; de Oliveira-Silva, R.; Sakellariou, D.; De Vos, D. E. Upcycling of Polystyrene to Aromatic Polyacids by Tandem Friedel–Crafts and Oxidation Reactions. *J. Am. Chem. Soc.* **2024**, *146*, 34753–34762. https://doi.org/10.1021/jacs.4c13265.
(14) Fukuda, O.; Sakaguchi, S.; Ishii, Y. Preparation of Hydroperoxides by *N*-Hydroxyphthalimide-Catalyzed Aerobic Oxidation of Alkylbenzenes and Hydroaromatic Compounds and Its Application. *Adv. Synth. Catal.* **2001**, *343*, 809–813. https://doi.org/10.1002/1615-4169(20011231)343:8<809::AID-ADSC809>3.0.CO;2-1.
(15) Melone, L.; Punta, C. *N*-Hydroxyphthalimide (NHPI)-Organocatalyzed Aerobic Oxidations: Advantages, Limits, and Industrial Perspectives. In *Liquid Phase Aerobic Oxidation Catalysis: Industrial Applications and Academic Perspectives*; John Wiley & Sons, Ltd, 2016; pp 253–265. https://doi.org/10.1002/9783527690121.ch16.
(16) Recupero, F.; Punta, C. Free Radical Functionalization of Organic Compounds Catalyzed by *N*- Hydroxyphthalimide. *Chem. Rev.* **2007**, *107*, 3800–3842. https://doi.org/10.1021/cr040170k.
(17) Yan, B.; Shi, C.; Beckham, G. T.; Chen, E. Y. -X.; Román-Leshkov, Y. Electrochemical Activation of C−C Bonds through Mediated Hydrogen Atom Transfer Reactions. *ChemSusChem* **2022**, *15*, e202102317. https://doi.org/10.1002/cssc.202102317.
(18) Ong, A.; Teo, J. Y. Q.; Feng, Z.; Tan, T. T. Y.; Lim, J. Y. C. Organocatalytic Aerobic Oxidative Degradation of Polystyrene to Aromatic Acids. *ACS Sustainable Chem. Eng.* **2023**, *11*, 12514–12522. https://doi.org/10.1021/acssuschemeng.3c01387.
(19) Partenheimer, W. Methodology and Scope of Metal/Bromide Autoxidation of Hydrocarbons. *Catal. Today* **1995**, *23*, 69–158. https://doi.org/10.1016/0920-5861(94)00138-R.
(20) Espenson, J. H.; Yiu, D. T.-Y. Kinetics and Activation Energy of the Oxidation of *para*-Tolyl Radical by Cobalt(III) in Acetic Acid: Competition Kinetics. *Int. J. Chem. Kinet.* **2005**, *37*, 599–604. https://doi.org/10.1002/kin.20116.
(21) Kushch, O.; Hordieieva, I.; Novikova, K.; Litvinov, Y.; Kompanets, M.; Shendrik, A.; Opeida, I. Kinetics of *N*-Oxyl

Radicals' Decay. *J. Org. Chem.* **2020**, *85*, 7112–7124. https://doi.org/10.1021/acs.joc.0c00506.

(22) Lopat'eva, E. R.; Krylov, I. B.; Subbotina, I. R.; Nikishin, G. I.; Terent'ev, A. O. Re-Examination of Self-Decay Chemistry of Phthalimide-*N*-Oxyl Redox-Organocatalyst for Free-Radical CH-Functionalization–Puzzle Begins to Come Together. *ChemCatChem* **2024**, *16*, e202400793. https://doi.org/10.1002/cctc.202400793.

(23) Hoyle, M.; Astbury, G. R. Investigation of the Flammability Limits of Acetic Acid at Elevated Temperature and Pressure. *Inst. Chem. Eng. Symp. Ser.* **1997**, *141*, 293–304.

(24) Osterberg, P. M.; Niemeier, J. K.; Welch, C. J.; Hawkins, J. M.; Martinelli, J. R.; Johnson, T. E.; Root, T. W.; Stahl, S. S. Experimental Limiting Oxygen Concentrations for Nine Organic Solvents at Temperatures and Pressures Relevant to Aerobic Oxidations in the Pharmaceutical Industry. *Org. Process Res. Dev.* **2015**, *19*, 1537–1543. https://doi.org/10.1021/op500328f.

(25) Crosby, G. A.; Kato, M. Halomethylation of Polystyrene. US3995094A, November 30, 1976. https://patents.google.com/patent/US3995094A/en (accessed 2025-01-16).

(26) Carpov, A.; Luca, C.; Bărboiu, V. On the Reaction of Linear and Crosslinked Polystyrene with 1,4-bis(Chloromethoxy)Butane. *J. Polym. Sci. Polym. Chem. Ed.* **1984**, *22*, 269–275. https://doi.org/10.1002/pol.1984.170220125.

(27) Warshawsky, A.; Deshe, A. Halomethyl Octyl Ethers: Convenient Halomethylation Reagents. *J. Polym. Sci. Polym. Chem. Ed.* **1985**, *23*, 1839–1841. https://doi.org/10.1002/pol.1985.170230623.

(28) Crounse, N. N. The Gattermann--Koch Reaction. The Formylation of Isopropylbenzene under Pressure. *J. Am. Chem. Soc.* **1949**, *71*, 1263–1264. https://doi.org/10.1021/ja01172a035.

(29) Sood, D. S.; Sherman, S. C.; Iretskii, A. V.; Kenvin, J. C.; Schiraldi, D. A.; White, M. G. The Formylation of Toluene in Trifluoromethanesulfonic Acid. *J. Catal.* **2001**, *199*, 149–153. https://doi.org/10.1006/jcat.2000.3144.

(30) Walter, H. A.; Blanchette, J. A. Preparation of Acetylated Styrene Polymers. US2962485A, November 29, 1960. https://patents.google.com/patent/US2962485A/en (accessed 2025-01-16).

(28) Sun, G.; Wheatley, W. B.; Worley, S. D. A New Cyclic *N*-Halamine Biocidal Polymer. *Ind. Eng. Chem. Res.* **1994**, *33*, 168–170. https://doi.org/10.1021/ie00025a022.

(32) Nasrullah, J. M.; Raja, S.; Vijayakumaran, K.; Dhamodharan, R. A Practical Route for the Preparation of Poly(4-Hydroxystyrene), a Useful Photoresist Material. *J. Polym. Sci. Part A: Polym. Chem.* **2000**, *38*, 453–461. https://doi.org/10.1002/(SICI)1099-0518(20000201)38:3<453::AID-POLA9>3.0.CO;2-6.

(33) For related observation of Co-free oxidation conditions, see ref. 13 and the following: Palumbo, C. T.; Gu, N. X.; Bleem, A. C.; Sullivan, K. P.; Katahira, R.; Stanley, L. M.; Kenny, J. K.; Ingraham, M. A.; Ramirez, K. J.; Haugen, S. J.; Amendola, C. R.; Stahl, S. S.; Beckham, G. T. Catalytic Carbon–Carbon Bond Cleavage in Lignin via Manganese–Zirconium-Mediated Autoxidation. *Nat Commun* **2024**, *15*, 862. https://doi.org/10.1038/s41467-024-45038-z.

(34) Prakash, G. K. S.; Yan, P.; Török, B.; Bucsi, I.; Tanaka, M.; Olah, G. A. Gallium(III) Trifluormethanesulfonate: A Water-Tolerant, Reusable Lewis Acid Catalyst for Friedel-Crafts Reactions. *Catal. Letters* **2003**, *85*, 1–6. https://doi.org/10.1023/A:1022133227407.

(35) Firouzabadi, H.; Iranpoor, N.; Nowrouzi, F. Aluminum Dodecatungstophosphate ($AlPW_{12}O_{40}$) as a Non-Hygroscopic Lewis Acid Catalyst for the Efficient Friedel–Crafts Acylation of Aromatic Compounds under Solvent-Less Conditions. *Tetrahedron* **2004**, *60*, 10843–10850. https://doi.org/10.1016/j.tet.2004.09.049.

(36) Manimaran, T.; Jr, A. E. H.; Lin, R. W.; Broeker, J. L.; Pahn, H. V.; Wiker, S. L. Reusable Friedel-Crafts Catalysts, Their Use, and Their Regeneration. WO2006022731A1, March 2, 2006. https://patents.google.com/patent/WO2006022731A1/en (accessed 2025-01-16).

(37) Alizadeh, A.; Khodaei, M. M.; Nazari, E. Silica Sulfuric Acid as an Efficient Solid Acid Catalyst for Friedel-Crafts Acylation Using Anhydrides. *Bull. Korean Chem. Soc.* **2007**, *28*, 1854–1856. https://doi.org/10.5012/BKCS.2007.28.10.1854.

(35) For related studies of MC oxidation of *p*-cymene under different conditions, see the following: Tibbetts, J. D.; Russo, D.; Lapkin, A. A.; Bull, S. D. Efficient Syntheses of Biobased Terephthalic Acid, *p*-Toluic Acid, and *p*-Methylacetophenone via One-Pot Catalytic Aerobic Oxidation of Monoterpene Derived Bio-*p*-Cymene. *ACS Sustainable Chem. Eng.* **2021**, *9*, 8642–8652. https://doi.org/10.1021/acssuschemeng.1c02605.

(39) Luo, Y.-R. *Comprehensive Handbook of Chemical Bond Energies*; CRC Press: Boca Raton, 2007. https://doi.org/10.1201/9781420007282.

TOC graphic

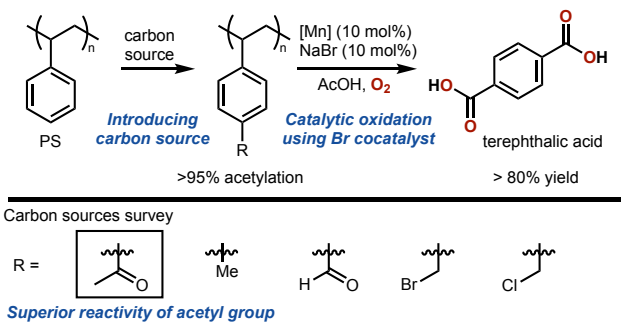
carbon source
[Mn] (10 mol%)
NaBr (10 mol%)
AcOH, O2
PS
Introducing carbon source
R
Catalytic oxidation using Br cocatalyst
terephthalic acid
>95% acetylation
> 80% yield
Carbon sources survey
R =
Me
Br
Cl
Superior reactivity of acetyl group

Supporting Information

Conversion of Polystyrene to Terephthalic Acid via Sequential Acetylation and Mn/Br-Catalyzed Autoxidation

Doohyun Baek,[a,b] Dylan J. Walsh,[a,b] James B. Gerken,[a] Madelyn G. Frank,[a] Ive Hermans,[a,b,c] and Shannon S. Stahl[a,b]*

[a]Department of Chemistry, University of Wisconsin−Madison,
Madison, Wisconsin 53706, United States

[b]The Wisconsin Energy Institute, University of Wisconsin−Madison,
Madison, Wisconsin 53726, United States

[c]Department of Chemical and Biological Engineering, University of Wisconsin−Madison,
Madison, Wisconsin 53706, United States

*stahl@chem.wisc.edu

Table of Contents:

1. General experimental considerations

1a. Materials and reagents

All reagents were purchased and used as received unless otherwise noted. *p*-cymene, *p*-isopropylbenzylchloride and cumene were purchased from TCI America. Polystyrene (M_w ~ 192 kDa), *p*-isoproylbenzaldehyde, *p*-toluic acid, *p*-methylacetophenone, diacetylbenzene, *p*-isopropylbenzoic acid, *p*-acetylbenzoic acid, terephthalic acid, cobalt(II) acetate tetrahydrate, manganese(II) acetate tetrahydrate, sodium bromide, *N*-methyl-*N*-(trimethylsilyl)trifluoroacetamide, aluminum chloride and acetyl chloride were purchased from Sigma Aldrich. *p*-isopropylbenzylbromide, *p*-isopropylacetophenone were purchased from Ambeed. All cobalt and manganese acetates used in this study were in their hydrated forms.

1b. Equipment and instrumentation

NMR spectra (^{1}H and ^{13}C) were obtained with either a Bruker Avance III 400 MHz spectrometer or a Bruker Avance III 500 MHz spectrometer referenced against the residual solvent peaks: $CDCl_3$ peaks at 7.26 ppm (^{1}H) and 77.16 ppm (^{13}C); $(CD_3)_2SO$ peaks at 2.50 ppm (^{1}H) and 39.52 ppm (^{13}C); multiplicities are described using the following abbreviations: s = singlet, d = doublet, dd = doublet of doublet, m = multiplet. High pressure oxidation reactions were performed with a 75 ml round-bottom glass pressure vessel (synthware, OD: 60 mm, Length: 139 mm, GL Thread: 15 mm) or a 300 mL titanium Parr reactor vessel with mechanical stirrer. PTFE tubing was purchased from Sigma-Aldrich (P_{max} = 500 psig, T_{max} = 250 °C). GPC analysis was performed using a Viscotek GPCmax/VE 2001 instrument fitted with set of two PolyPore columns (molecular weight range: 500-400,000). Polymer samples were prepared with THF (concentration: 2.5 mg/mL) then injected at a flow rate of 1 mL/min at 40 °C. Polymers were characterized by their refractive index (RI) using a Viscotek model 302-050 tetra detector array. Omnisec software (Viscotek, Inc.) was used for initial data processing such as baseline correction and applying molecular weight calibrations. Molecular weight calibrations were determined using polystyrene standards (MW 580–364,000 Da). Fourier-transform infrared (FTIR) spectra were obtained by using diamond crystal attenuated total reflection (ATR) geometry on a Bruker Tensor 27 spectrometer at room temperature. Scan range was 4000–600 cm^{-1} and accumulations of 32 scans.

Gas chromatography experiments were performed using an Agilent 8890 GC system coupled to 5977C mass spectrometer and fitted with an DB-35ms Ultra Inert column (30 m, 0.320 mm, 0.25 μm; Part No. 123-3832UI). Helium gas was used as a carrier gas. Samples were injected in at an injector temperature of 250 °C. The oven temperature program profile was as follows: column oven was kept at 50 C° for 3 min (initial temperature) and increased at 8 C°/min to 150 C°, and 15 C°/min to 300 C°.

Qualitative GC-MS analysis was performed with Agilent 8890 GC system equipped with MS 5977C (electron ionization (EI) mode) to identify the products using 'Agilent MassHunter Qualitative Analysis 10.0' software. After identifying the products, quantitative analysis was performed with flame ionization detectors (FID) signal by using the effective carbon number (ECN) concept[1] to calculate the yields of products.

1c. Safety considerations

I. The reagents (cumene, *p*-cymene, *p*-isopropylacetophenone) used in this paper can form benzylic hydroperoxides, which are potentially explosive. These reagents were tested for peroxides prior to use.

II. The oxidation conditions employed in this study (e.g., 100 psi O_2) exceed the experimental limiting oxygen concentration (LOC) for safe aerobic oxidation. For reference, the LOC of acetic acid is reported as 9.6 vol% at 20 bar and 200 °C.[2] These limits were exceeded in our small scale experiments in order to avoid excessively high pressures associated with use of dilute O_2, which also represents a safety hazard. To mitigate associated safety risks, all oxidation reactions were conducted in pressure reactors equipped with double blast shields and pressure relief valves. Larger scale reactions should not be conducted without conducting full safety review.

III. The use of $AlCl_3$ and AcCl generates HCl, and the use of NaBr produces Br radicals and HBr. In both cases, a glass or titanium reactor is required to prevent corrosion and reactor damage.

.

2. General experimental procedure

2a. General experimental procedure with pressure reactor (glass reactor)

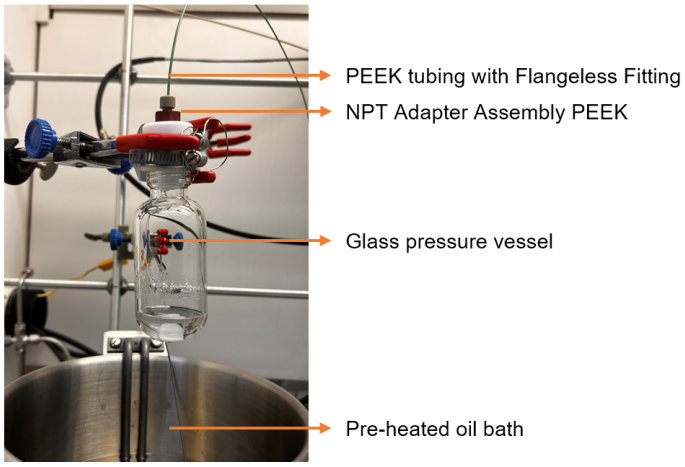

Figure S1. Glass pressure reactor setup.

Reactor setup: The 75 mL glass pressure vessel (Synthware, OD: 60 mm, Length: 139 mm, GL Thread: 15 mm) was equipped with custom-made cap which is equipped with NPT Adapter Assembly PEEK (1/8 inch NPT male x 1/4 inch female) and connected to the O_2 cylinder using the PEEK tubing equipped with Idex Flangeless Fitting (1/8 inch). Idex back pressure regulator was equipped into the O_2 line for additional safety.

Reaction setup: To the vessels were added sequentially: a magnetic stir bar, substrate (1.50 mmol), $Co(OAc)_2$•$4H_2O$ (18.7 mg, 0.075 mmol), $Mn(OAc)_2$•$4H_2O$ (18.4 mg, 0.075 mmol or 36.8 mg, 0.15 mmol), NaBr (15.4 mg, 0.15 mmol) and AcOH (15.0 mL). The vessel was pressurized with O_2 (100 psi). The mixture was stirred at 500 rpm in a pre-heated oil bath.

Reaction quench: After 1 h, the vessel was cooled down to 0 °C with ice bath and depressurized. *p*-Terephthalic acid was simply isolated by filtration without further purification. From the filtrate, 25 µL aliquot was removed to the separated GC 2 mL vial equipped with 350 µL glass flat insert, and mixed with 100 µL of *N*-methyl-*N*-(trimethylsilyl)trifluoroacetamide for trimethylsilylation of aromatic carboxylic acid products. After 2 h, 25 µL of a stock solution (prepared by dissolving 5.001 g of 1,3-dichlorobenzene in 450.24 g of ethyl acetate; 6.8 mM) of the internal standard was added into the vial. Then, 200 µL of ethyl acetate was added to dilute the sample. GC/MS analysis was performed with the prepared vial sample.

2b. General experimental procedure with Parr reactor (titanium reactor)

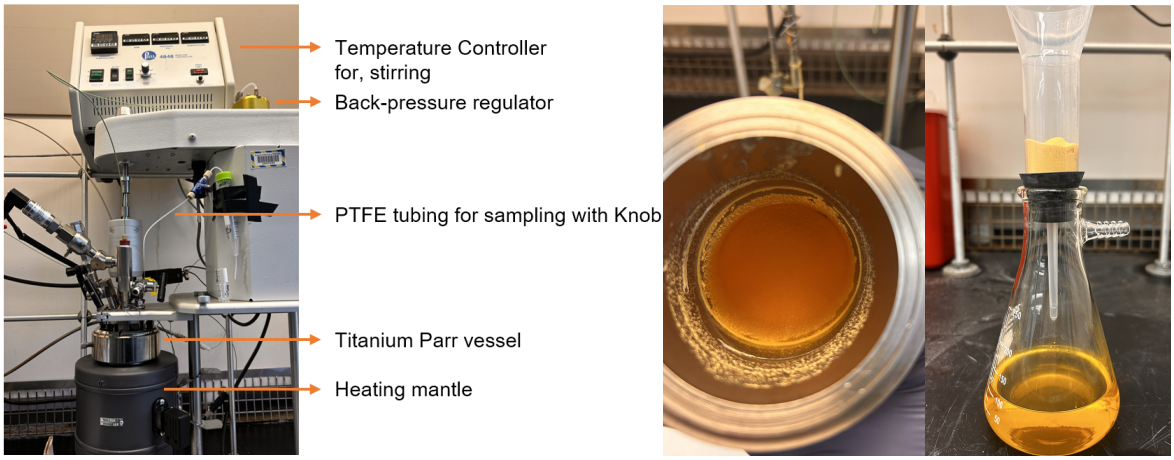

Figure S2. Titanium Parr reactor setup.

Reactor setup: The titanium Parr reactor vessel was equipped with heating mantle. Zaiput back-pressure regulator (200 psi, N_2) was coupled into the reactor to make continuous O_2 flow environment at 200 psi. Additionally, PTFE tubing with knob was inserted into the reactor to collect reaction mixture during the MC oxidation reaction.

Reaction setup: To the vessels were added sequentially: substrates (30.0 mmol), $Co(OAc)_2•4H_2O$ (373.6 mg, 1.50 mmol), $Mn(OAc)_2•4H_2O$ (367.6 mg, 1.50 mmol or 735 mg, 3.0 mmol), NaBr (308.7 mg, 3.0 mmol) and AcOH (100 mL). The vessel was pressurized with O_2 (200 psi). The mixture was stirred at 500 rpm and heated to desired temperature by temperature controller.

Reaction quench: After 1 h, the vessel was cooled down to 0 °C with ice bath and depressurized. *p*-Terephthalic acid was simply isolated by filtration without further purification. From the filtrate, 25 µL aliquot was removed to the separated GC 2 mL vial equipped with 350 µL glass flat insert, and mixed with 100 µL of *N*-methyl-*N*-(trimethylsilyl)trifluoroacetamide. After 2 h, 25 µL of a stock solution (prepared by dissolving 5.001 g of 1,3-dichlorobenzene in 450.24 g of ethyl acetate; 6.8 mM) of the internal standard was added into the vial. Then, 200 µL of ethyl acetate was added to dilute the sample. GC/MS analysis was performed with the prepared vial sample.
For time-course study, approximately 50-80 µL of crude mixture was collected by the PTFE tubing at each time point, and 25 µL aliquot was removed to the separated GC 2 mL vial equipped with 350 µL glass flat insert and mixed with 100 µL of *N*-methyl-*N*-(trimethylsilyl)trifluoroacetamide. After 2 h, 25 µL of a stock solution (prepared by dissolving 5.001 g of 1,3-dichlorobenzene in 450.24 g of ethyl acetate; 6.8 mM) of the internal standard was added into the vial. Then, 200 µL of ethyl acetate was added to dilute the sample. GC/MS analysis was performed with the prepared vial sample.

2c. General experimental procedure with flow reactor

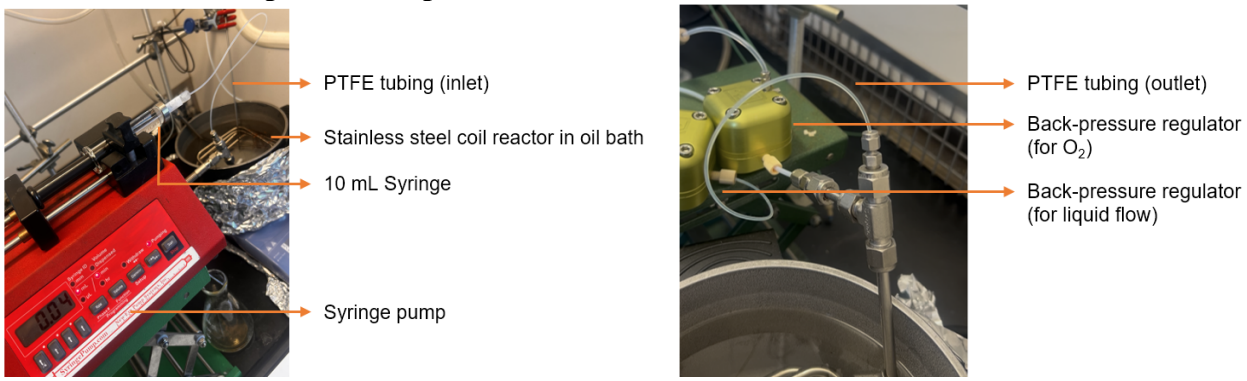

Figure S3. Flow reactor setup.

Reactor setup: The oxidation was carried out in a flow reactor equipped with a 1 mL stainless steel coil containing PTFE tubing. Two Zaiput back-pressure regulators were connected to the system for O_2 and liquid flow. The coil was heated using an oil bath. The reaction mixture was delivered using a 10 mL Hamilton Gastight Luer Lock syringe driven by a syringe pump. The back-pressure regulators were modified to enable continuous flow without air bubbles in the tubing (Optimized setup: back-pressure regulator for O_2: 80 psi, back-pressure regulator for liquid flow: 80 psi).

Reaction setup: To the 20 mL vial were added sequentially: substrate (1.50 mmol), $Mn(OAc)_2$•$4H_2O$ (36.8 mg, 0.15 mmol), NaBr (15.4 mg, 0.15 mmol) and AcOH (15.0 mL). 10 mL of the reaction mixture in the vial were drawn into a Hamilton Gastight Luer Lock syringe, which was then mounted on a syringe pump for delivery. The reaction was initiated by turning on the syringe pump, and samples were collected at different time points by adjusting the flow rate. (For example, a flow rate of 1 mL/min corresponds to a 1 min residence time in the 1 mL flow reactor.)

Reaction quench: For time-course study, approximately 50-80 µL of crude mixture was collected from the PTFE tubing outlet at each time point, and 25 µL aliquot was removed to the separated GC 2 mL vial equipped with 350 µL glass flat insert, and mixed with 100 µL of *N*-Methyl-*N*-(trimethylsilyl)trifluoroacetamide. After 2 h, 25 µL of a stock solution (prepared by dissolving 5.001 g of 1,3-dichlorobenzene in 450.24 g of ethyl acetate; 6.8 mM) of the internal standard was added into the vial. Then, 200 µL of ethyl acetate was added to dilute the sample. GC/MS analysis was performed with the prepared vial sample.

3. Reaction optimization

3a. Reaction time-course study of Co/Mn/NHPI vs Co/Mn/Br catalytic system

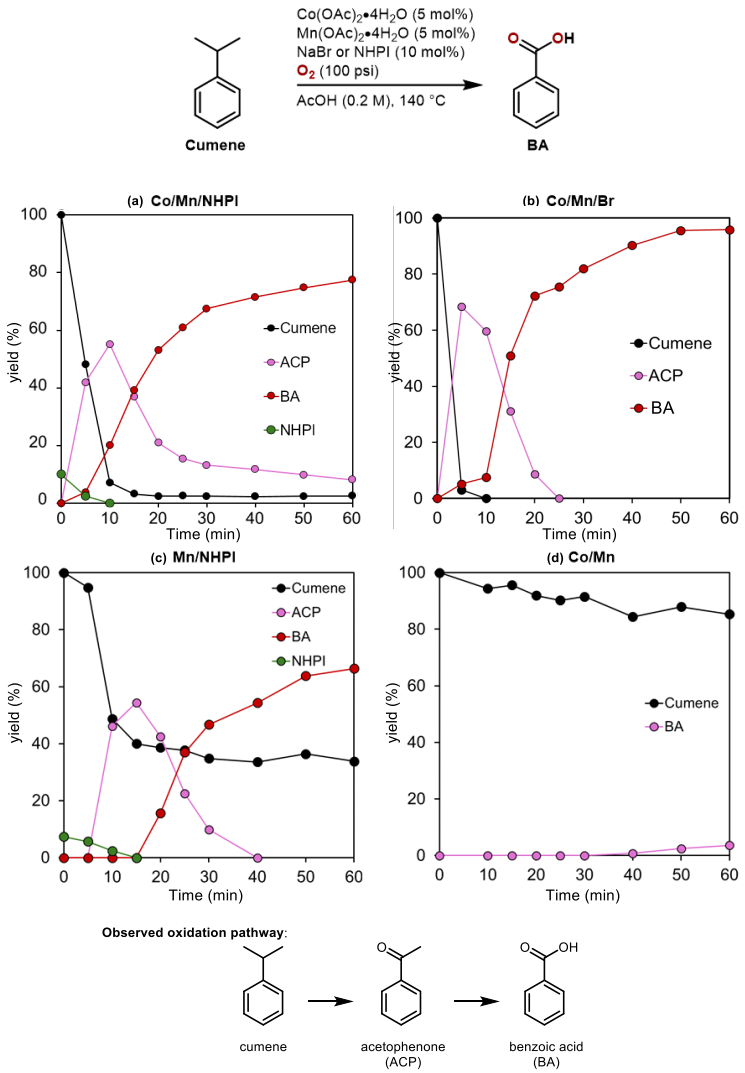

Figure S4. Reaction time-course study using different catalytic systems under the following reaction conditions: (a) Co/Mn/NHPI (5/5/10 mol%, same data as **Figure 2** of the main manuscript) (b) Co/Mn/Br (5/5/10 mol%, same data as **Figure 2** of the main manuscript) (c) Mn/NHPI (10/10 mol%) (d) Co/Mn (5/5 mol%).

The reaction was set up and analyzed following the general experimental procedure (**section 2a** of Supporting Information), using a glass reactor. NHPI decomposed in less than 10 minutes under the Co/Mn/NHPI conditions (**Figure S4a**), with only a small amount of acetophenone remaining. Under Co/Mn/Br conditions, cumene was fully converted to acetophenone and subsequently to benzoic acid (**Figure S4b**). The decomposition of NHPI was slower under the Mn/NHPI conditions (**Figure S4c**), but still occurred within 20 minutes. In the absence of NHPI or a Br promoter, trace benzoic acid was formed within 60 min.

3b. MC oxidation reaction optimization with compound 5

Table S1. Catalysts screening for the MC oxidation of compound **5**.

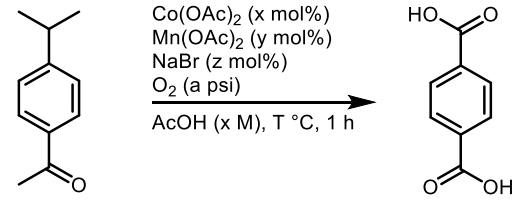

5 (1.5 mmol) → TA

Entry	Catalysts [mol%]	Conc. [M]	O_2 condition	Temp. [°C]	Yield [%]
1	Co/Mn/Br = 1/1/2	0.1	100 psi	160	39
2	Co/Mn/Br = 2/2/4	0.1	100 psi	160	67
3	Co/Mn/Br = 5/5/10	0.1	100 psi	160	71
4	Mn/Br = 10/10	0.1	100 psi	160	76
5	Mn/Br = 10/10	0.3	100 psi	160	79
6	Mn/Br = 10/10	1.0	100 psi	160	78
7	Mn/Br = 10/10	0.3	100 psi	180	81
8	Mn/Br = 10/10	0.3	200 psi	180	82

The reaction was set up and analyzed according to the general experimental procedure described in **Section 2** of the Supporting Information, using a glass reactor (entries 1–7) or a titanium reactor (entry 8) with varying catalyst loadings and concentrations.

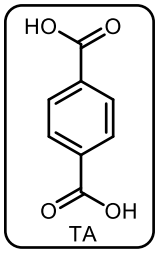

^{1}H-NMR (500 MHz, DMSO) δ 8.04 (s, 4H)
^{13}C-NMR (126 MHz, DMSO) δ 166.75, 134.49, 129.55

4. Experimental procedure of polystyrene acetylation and oxidation

4a. Synthesis of acetylated polystyrene

Scheme S1. Synthesis of acetylated polystyrene.

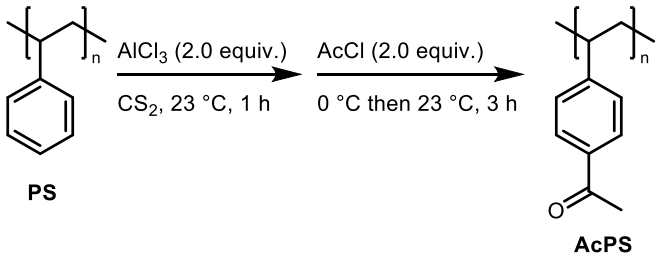

Acetylated polystyrene (AcPS) was prepared by following previous literature.[3] To a flame-dried Schlenk flask charged with a stir bar, polystyrene (2.08 g, 20 mmol) was fully dissolved in 300 mL of CS_2 and $AlCl_3$ (5.3 g, 40 mmol, 2.0 equiv.) was added in one portion at 0 °C. The mixture was warmed to 23 °C under vigorous stirring for 1 h. Acetyl chloride (2.9 mL, 40 mmol, 2.0 equiv.) was added in the mixture dropwise and stirred for additional 3 h. The reaction mixture was added to ice followed by the addition of concentrated HCl (50 mL). 100 mL of CS_2 was added into the crude mixture, and transferred to a separatory funnel. Organic layer was collected and evaporated, then re-dissolved in 50 mL of THF. The crude mixture was precipitated into excess methanol (200 mL), and dried under vacuum to afford desired product (AcPS, 2.52 g, 95% acetylation ratio by ^{1}H NMR, 88% mass recovery).

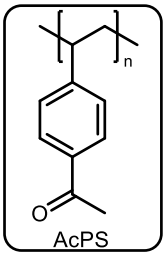

Acetylated polystyrene (AcPS)
^{1}H-NMR (500 MHz, $CDCl_3$) δ 7.28-7.75 (br m, 2H), 6.15-7.16 (br m, 2H) 2.49 (br s, 3H) 1.10-2.15 (br m, 3H)

The NMR spectra matched with previously reported literature.[3,4]

Calculation of the acetylation (%): The acetylation ratio was calculated by ^{1}H NMR, as described in **Figure 4b**.

$$Acetylation\ (\%) = \frac{The\ integrals\ of\ metyhl\ protons\ of\ the\ acetyl\ group}{The\ integrals\ of\ benzylic\ and\ methylene\ protons\ of\ the\ backbone} = \frac{1.00}{1.05} = 95\%$$

Calculation of the mass recovery (%): The average molar mass (M_{avg}) of the 95% acetylated polystyrene was calculated according to a previously reported procedure.[4]

$$M_{avg} = 146\ \left(\frac{g}{mol}\right) \times 0.95\ + 104\left(\frac{g}{mol}\right) \times 0.05 = 143.9\ \left(\frac{g}{mol}\right)$$

Starting mmol of polystyrene = 20 mmol = 0.02 mol

Theoretical maximum mass of 95% acetylated polystyrene = $143.9\ \left(\frac{\text{g}}{\text{mol}}\right) \times 0.02$ = 2.88 g

Experimental mass of 95% acetylated polystyrene = 2.52 g

$$Mass\ recovery\ (\%) = \frac{Experimental\ mass}{Theoretical\ maximum\ mass} = \frac{2.52}{2.88} = 88\%$$

4b. Additional screening for catalytic acetylation of polystyrene

Table S2. Additional screening for catalytic acetylation of polystyrene using acetic anhydride (Ac_2O, left column) and acetyl chloride (AcCl, right column).

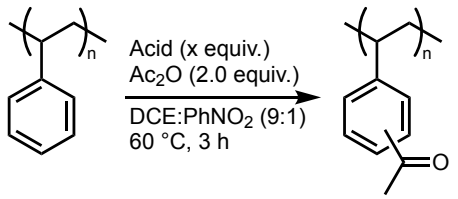

Entry	Acids (equiv.)	Acetylation ratio (%)
1	SiO_2-OSO_3H (100 wt%)	N.D.
2	SiO_2-$AlCl_3$ (100 wt%)	N.D.
3	Fe_2O_3 (1.0 equiv.)	N.D.
4	ZnO (1.0 equiv.)	N.D.
5	$AlPO_{12}W_{40}$ (100 wt%)	N.D.
6	$H_3PO_{12}W_{40}$ (100 wt%)	N.D.
7	Ga $(OTf)_3$ (0.5 equiv.)	N.D.
8	$Ga(OTf)_3$ (1.0 equiv.)	N.D.
9	$NaFeCl_4$ (1.0 equiv.)	N.D.

N.D.=Not detected

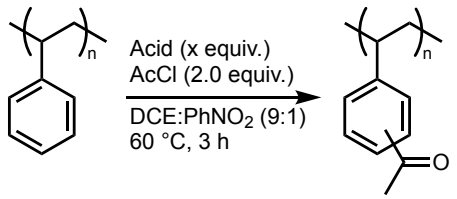

Entry	Acids (equiv.)	Acetylation ratio (%)
1	SiO_2-OSO_3H (100 wt%)	N.D.
2	SiO_2-$AlCl_3$ (100 wt%)	N.D.
3	Fe_2O_3 (1.0 equiv.)	N.D.
4	ZnO (1.0 equiv.)	5
5	$AlPO_{12}W_{40}$ (100 wt%)	N.D.
6	$H_3PO_{12}W_{40}$ (100 wt%)	N.D.
7	Ga $(OTf)_3$ (0.5 equiv.)	6
8	$Ga(OTf)_3$ (1.0 equiv.)	8
9	$NaFeCl_4$ (1.0 equiv.)	Crosslinking

N.D.=Not detected

To a flame-dried Schlenk flask charged with a stir bar and polystyrene (208 mg, 2.0 mmol), fully dissolved in 10 mL of DCE:$PhNO_2$ (9:1), catalysts (as marked in Table S2) was added in one portion at 0 °C. The mixture was warmed to 23 °C under vigorous stirring for 1 h. Acetyl chloride (285 μL, 4.0 mmol, 2.0 equiv.) was added in the mixture and stirred for additional 3 h. The reaction mixture was added to ice followed by the addition of concentrated HCl (5 mL). 10 mL of DCE:$PhNO_2$ (9:1) was added into the crude mixture, and put into separatory funnel. Organic layer was collected and evaporated, then re-dissolved in 5 mL of THF. The crude was precipitated into excess methanol (20 mL), and dried under vacuum to afford desired product. Acetylation ratio was calculated by ^{1}H NMR.

4c. Early reaction time point using flow reactor

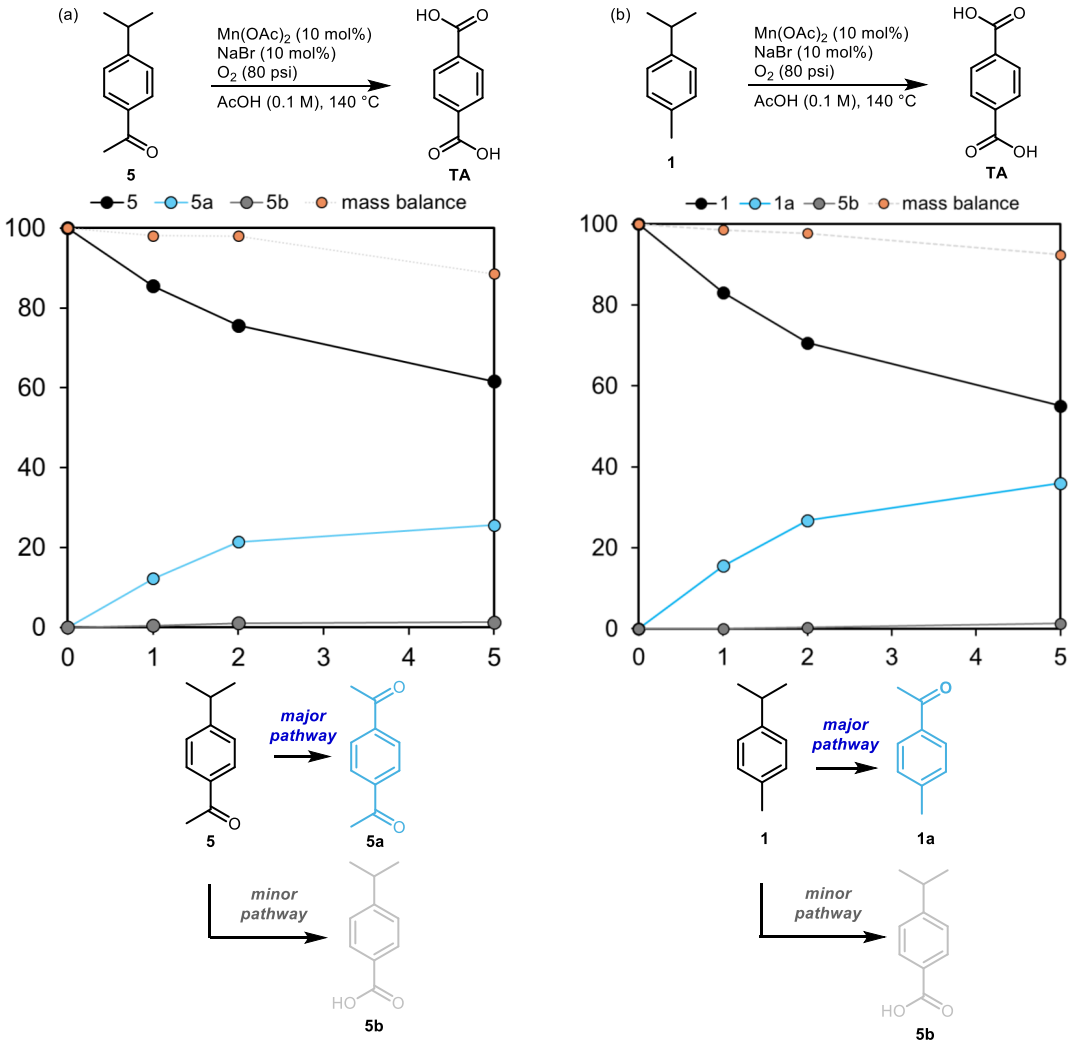

Figure S5. Time-course reaction profile of the oxidation reaction of **1** (a) and **5** (b) using flow reactor.

To clarify the major oxidation pathways of compounds **1** and **5**, early reaction time points (<10 min) were investigated. A flow reactor was selected for these experiments, as the glass reactor and titanium Parr reactor were not suitable for capturing early time points due to delayed heat transfer and temperature equilibration. The reaction was set up and analyzed following the general experimental procedure (**section 2c** of Supporting Information). At the 1 min and 2 min time points, compound **1** was clearly oxidized to **1a** with high mass balance. Similarly, compound **5** was oxidized to **5a** with high mass balance at the early reaction time points, indicating that **1a** and **5a** are the major products formed through the primary oxidation pathways.

4d. Oxidation of acetylated polystyrene

Scheme S2. MC oxidation of AcPS to aromatic oxygenates.

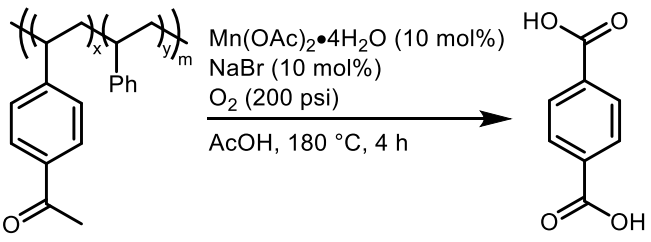

AcPS **TA**

Reaction setup: To the vessels were added sequentially: AcPS (2.52 g, synthesized from **section 4a**), $Mn(OAc)_2•4H_2O$ (409.3 mg, 1.67 mmol), NaBr (171.8 mg, 1.67 mmol) and AcOH (100 mL). The vessel was pressurized with O_2 (200 psi). The mixture was stirred at 500 rpm and heated to 180 °C by temperature controller system.

Reaction quench: After 1 h, the vessel was cooled down to 0 °C with ice bath and depressurized. *p*-Terephthalic acid was simply isolated by filtration without further purification (13.4 mmol, 81% yield).

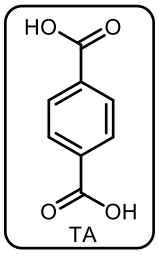

^{1}H-NMR (500 MHz, DMSO) δ 8.04 (s, 4H)
^{13}C-NMR (126 MHz, DMSO) δ 166.75, 134.49, 129.55

Side product analysis

I. Analytic method for precipitate (terephthalic acid)

The filtered precipitate (10 mg) was treated with 200 µL of *N*-methyl-*N*-(trimethylsilyl)trifluoroacetamide and heated at 60 °C for 3 h. Once a homogeneous solution was obtained, 25 µL aliquot was removed to the separated GC 2 mL vial equipped with 350 µL glass flat insert. Then, 25 µL of a stock solution (prepared by dissolving 5.001 g of 1,3-dichlorobenzene in 450.24 g of ethyl acetate; 6.8 mM) of the internal standard was added into the vial. Then, 200 µL of ethyl acetate was added to dilute the sample. GC/MS analysis was performed with the prepared vial sample. Phthalic acid (0.01 mmol, 0.08%) was observed as a side product in the precipitate. The primary impurity formed in the reaction is benzoic acid, but it remains soluble in AcOH and is only detected in the filtrate (see below).

II. Analytic method for filtrate

From the filtrate, 25 µL aliquot was removed to the separated GC 2 mL vial equipped with 350 µL glass insert and mixed with 100 µL of *N*-methyl-*N*-(trimethylsilyl)trifluoroacetamide for trimethylsilylation of aromatic carboxylic acid products. After 2 h, 25 µL of a stock solution (prepared by dissolving 5.001 g of 1,3-dichlorobenzene in 450.24 g of ethyl acetate; 6.8 mM) of the internal standard was added into the vial. Then, 200 µL of ethyl acetate was added to dilute the sample. GC/MS analysis was performed with the prepared vial sample. Benzoic acid (0.51 mmol) was observed as side product in the filtrate.

4e. Application to post-consumer polystyrene products

Scheme S3. Acetylation and subsequent oxidation of post-consumer polystyrene.

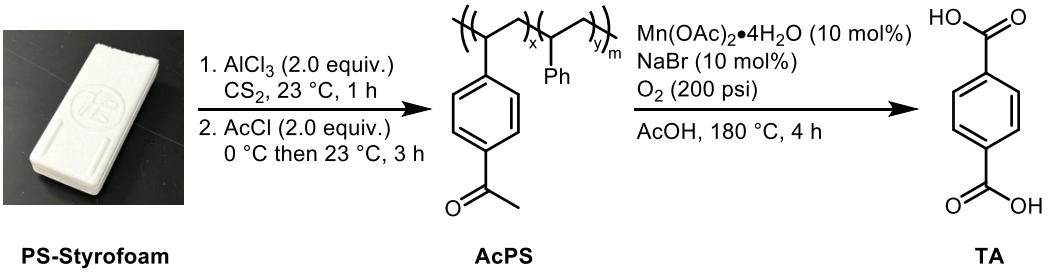

To a flame-dried Schlenk flask charged with a stir bar, post-consumer polystyrene (Styrofoam, 2.08 g, 20 mmol) was fully dissolved in 300 mL of CS_2 and $AlCl_3$ (5.3 g, 40 mmol, 2.0 equiv.) was added in one portion at 0 °C. The mixture was warmed to 23 °C under vigorous stirring for 1 h. Acetyl chloride (2.9 mL, 40 mmol, 2.0 equiv.) was added in the mixture dropwise and stirred for additional 3 h. The reaction mixture was added to ice followed by the addition of concentrated HCl (50 mL). 100 mL of CS_2 was added into the crude mixture, and transferred to a separatory funnel. Organic layer was collected and evaporated, then re-dissolved in 50 mL of THF. The crude mixture was precipitated into excess methanol (200 mL), and dried under vacuum to afford desired product (AcPS, 2.12 g, 93% acetylation ratio by ^{1}H NMR, 74% mass recovery).

To the titanium reactor vessels were added sequentially: AcPS (2.12 g), $Mn(OAc)_2$•$4H_2O$ (335.8 mg, 1.37 mmol), NaBr (141.0 mg, 1.37 mmol) and AcOH (100 mL). The vessel was pressurized with O_2 (200 psi). The mixture was stirred at 500 rpm and heated to 180 °C by temperature controller system. After 1 h, the vessel was cooled down to 0 °C with ice bath and depressurized. *p*-Terephthalic acid was simply isolated by filtration without further purification (9.61 mmol, 70% yield).

5. Characterization of acetylated polystyrene

5a. IR spectrum of acetylated polystyrene

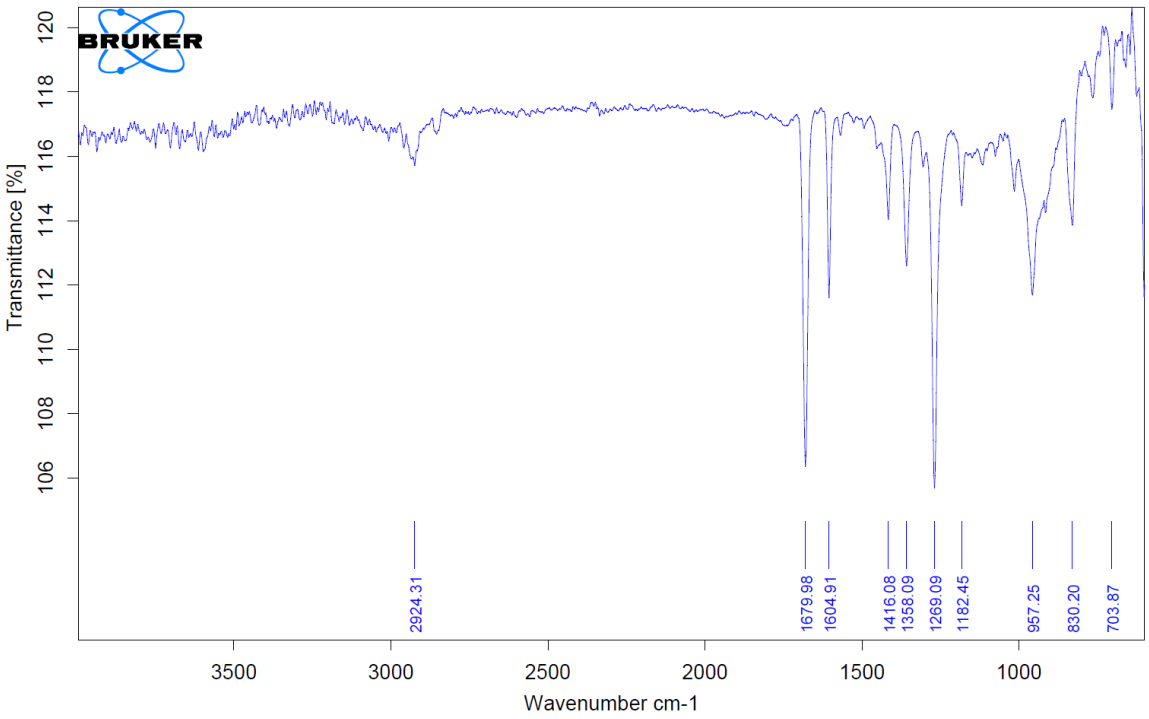

Figure S6. IR spectrum of acetylated polystyrene.

5b. GPC analysis of acetylated polystyrene

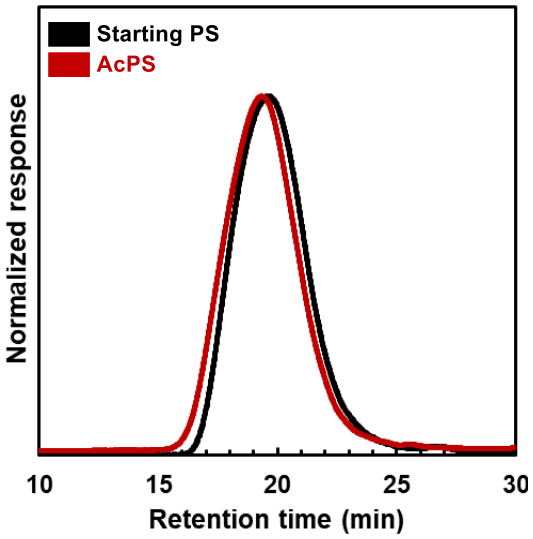

Entry	Peak position (min)	M_w (kDa)	M_n (kDa)	PDI (M_w/M_n)
Starting PS	19.53	180	59	3.1
AcPS	20.74	233	64	3.6

Figure S7. GPC analysis of acetylated polystyrene.

6. References

(1) Scanlon, J. T.; Willis, D. E. Calculation of Flame Ionization Detector Relative Response Factors Using the Effective Carbon Number Concept. *J. Chromatogr. Sci.* **1985**, *23*, 333–340. https://doi.org/10.1093/chromsci/23.8.333.

(2) Osterberg, P. M.; Niemeier, J. K.; Welch, C. J.; Hawkins, J. M.; Martinelli, J. R.; Johnson, T. E.; Root, T. W.; Stahl, S. S. Experimental Limiting Oxygen Concentrations for Nine Organic Solvents at Temperatures and Pressures Relevant to Aerobic Oxidations in the Pharmaceutical Industry. *Org. Process Res. Dev.* **2015**, *19*, 1537–1543. https://doi.org/10.1021/op500328f.

(3) Nasrullah, J. M.; Raja, S.; Vijayakumaran, K.; Dhamodharan, R. A Practical Route for the Preparation of Poly(4-Hydroxystyrene), a Useful Photoresist Material. *J. Polym. Sci. Part A: Polym. Chem.* **2000**, *38*, 453–461. https://doi.org/10.1002/(SICI)1099-0518(20000201)38:3<453::AID-POLA9>3.0.CO;2-6.

(4) Giakoumakis, N. S.; Marquez, C.; de Oliveira-Silva, R.; Sakellariou, D.; De Vos, D. E. Upcycling of Polystyrene to Aromatic Polyacids by Tandem Friedel–Crafts and Oxidation Reactions. *J. Am. Chem. Soc.* **2024**, *146*, 34753–34762. https://doi.org/10.1021/jacs.4c13265.

7. NMR Spectra

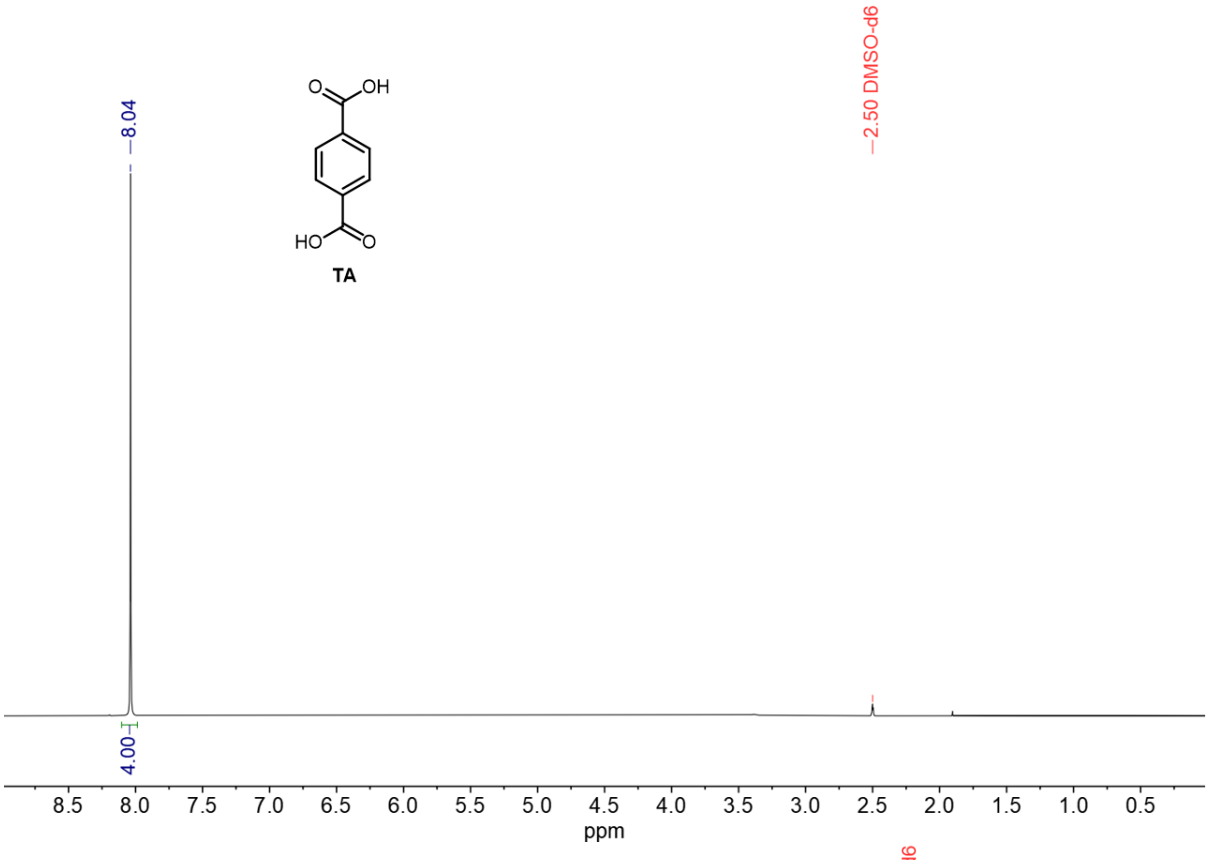

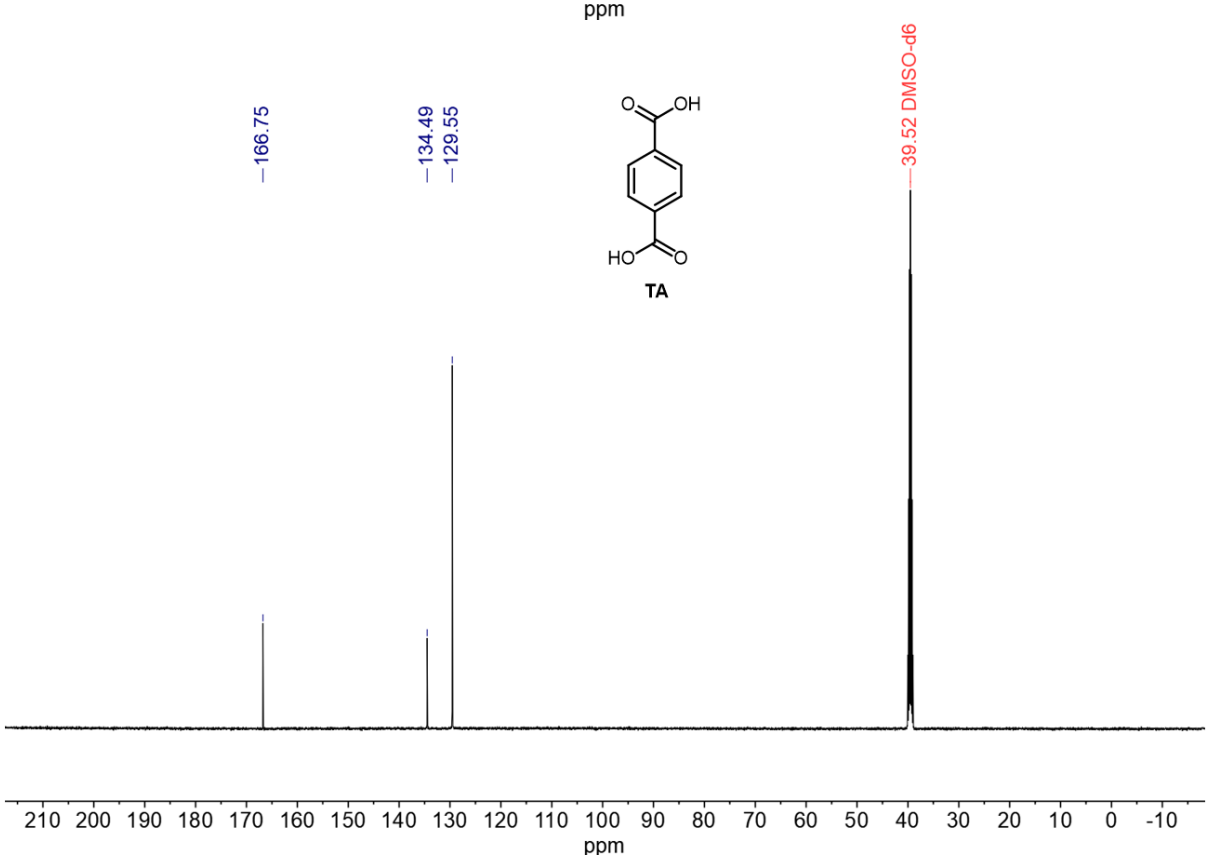

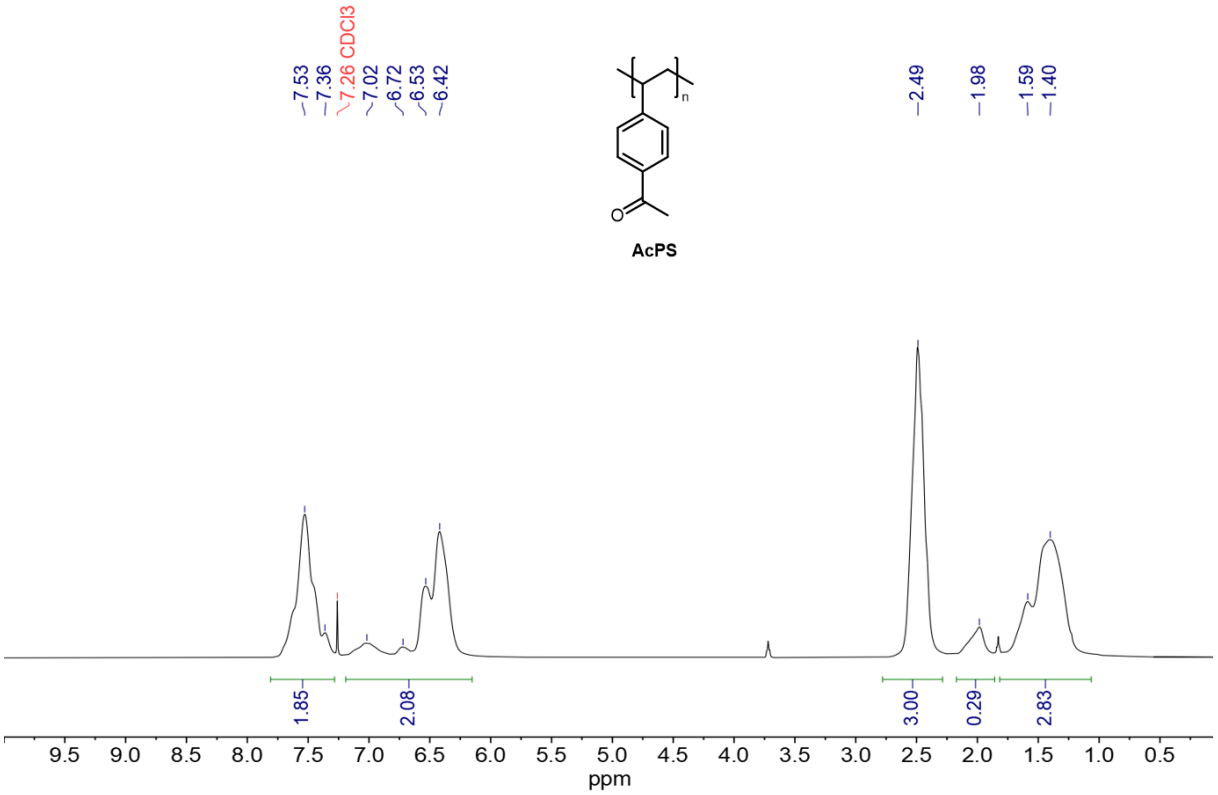
7.53
7.36
7.26 CDCl3
7.02
6.72
6.53
6.42
2.49
1.98
1.59
1.40
n
O
AcPS
1.85
2.08
3.00
0.29
2.83
9.5 9.0 8.5 8.0 7.5 7.0 6.5 6.0 5.5 5.0 4.5 4.0 3.5 3.0 2.5 2.0 1.5 1.0 0.5
ppm